



Article

The Utility of Sentinel-2 Spectral Data in Quantifying Above-Ground Carbon Stock in an Urban Reforested Landscape

Mthembeni Mngadi *, John Odindi and Onesimo Mutanga

Discipline of Geography, School of Agricultural, Earth and Environmental Sciences,
University of KwaZulu-Natal, Pietermaritzburg 3201, South Africa; odindi@ukzn.ac.za (J.O.);
MutangaO@ukzn.ac.za (O.M.)

* Correspondence: 212518076@stu.ukzn.ac.za; Tel.: +27-76-070-5077

Abstract: The transformation of the natural landscape into an impervious surface due to urbanization has often been considered an important driver of environmental change, affecting essential urban ecological processes and ecosystem services. Continuous forest degradation and deforestation due to urbanization have led to an increase in atmospheric carbon emissions, risks, and impacts associated with climate change within urban landscapes and beyond them. Hence, urban reforestation has become a reliable long-term alternative for carbon sink and climate change mitigation. However, there is an urgent need for spatially accurate and concise quantification of these forest carbon stocks in order to understand and effectively monitor the accumulation and progress on such ecosystem services. Hence, this study sought to examine the prospect of Sentinel-2 spectral data in quantifying carbon stock in a reforested urban landscape using the random forest ensemble. Results show that Sentinel-2 spectral data estimated reforested forest carbon stock to an RMSE between 0.378 and 0.466 t·ha⁻¹ and R² of 79.82 and 77.96% using calibration and validation datasets. Based on random forest variable selection and backward elimination approaches, the red-edge normalized difference vegetation index, enhanced vegetation index, modified simple ratio index, and normalized difference vegetation index were the best subset of predictor variables of carbon stock. These findings demonstrate the value and prospects of Sentinel-2 spectral data for predicting carbon stock in reforested urban landscapes. This information is critical for adopting informed management policies and plans for optimizing urban reforested landscapes carbon sequestration capacity and improving their climate change mitigation potential.

Keywords: reforestation; ecosystem services; carbon stock; random forest



Citation: Mngadi, M.; Odindi, J.; Mutanga, O. The Utility of Sentinel-2 Spectral Data in Quantifying Above-Ground Carbon Stock in an Urban Reforested Landscape. *Remote Sens.* **2021**, *13*, 4281. <https://doi.org/10.3390/rs13214281>

Academic Editor: Peng Fu

Received: 19 August 2021

Accepted: 19 October 2021

Published: 25 October 2021

Publisher's Note: MDPI stays neutral with regard to jurisdictional claims in published maps and institutional affiliations.



Copyright: © 2021 by the authors. Licensee MDPI, Basel, Switzerland. This article is an open access article distributed under the terms and conditions of the Creative Commons Attribution (CC BY) license (<https://creativecommons.org/licenses/by/4.0/>).

1. Introduction

Urbanization, typified by transformation of natural landscape into impervious built-up surfaces, is considered a major driver of environmental change [1–3]. Such transformation significantly affects the integrity of important ecological processes and ecosystem services that include deterioration of water quality, increase in urban thermal heat, air and noise pollution, loss of biodiversity, and acceleration of climate change [3–5]. Despite covering small land-surface, urban areas account for the highest amount of global carbon emissions due to higher energy and resource consumption [6]. Commonly, urban vegetation (especially forest ecosystems) sequester the emitted carbon and regulate climate systems within urban landscapes. However, deforestation and forest degradation that typifies urbanization processes reduces urban areas' carbon sequestration potential and increases greenhouse gas accumulations [7–10]. In sub-Saharan Africa for instance, studies show that urbanization exert enormous pressure on the spatial distribution of urban forest ecosystems, hence decreasing substantial amount of sequestered carbon and accelerate potential risks and impacts of climate change [11,12].

Recently, the United Nations Framework Convention for Climate Change (UNFCCC) established the Reducing Emissions from Deforestation and forest Degradation (REDD+)

that requires countries to report their carbon emissions and sink estimates through national greenhouse gas inventories (NGHGI) [13,14]. Furthermore, the REDD+ and Kyoto Protocol programs have identified reforestation initiatives as the most efficient, low-cost, and long-term approach for reducing greenhouse gas emissions and climate change impacts, especially in urban landscapes [3,4]. The emergence and recognition of reforestation as the potential carbon sink in urban landscapes is expected to significantly influence the global carbon cycle, improve urban environmental quality, and regulate climate systems. Subsequently, an explicit investigation in the methods and procedures for quantifying these carbon emissions and sinks is paramount.

Numerous studies have assessed regulating ecosystem services such as carbon stock or sequestration and aboveground biomass [15–17]. However, existing assessments are biased towards natural/indigenous and commercial forests. Despite the need for knowledge on the contribution of urban reforestation on the global carbon cycle and climate change regulation potential, information on carbon stocks in reforested urban areas remain largely unknown. Hence, there is a need to establish affordable, spatially explicit and robust techniques, as well as datasets to effectively quantify and monitor carbon stocks in urban reforested landscapes.

Traditionally, field surveys have been used to determine aboveground carbon [18,19]. Whereas field surveys and observations are known to be highly accurate, their shortcomings are widely documented in the available literature [16,20]. Meanwhile, among others, the Inter-Governmental Panel on Climate Change Good Practice Guidance (IPCC-GPG) on Land Use, Land Use Change, and Forestry has proposed remote sensing as a cost-effective and reliable primary data source and technique for wall-to-wall mapping and estimation of forest carbon dynamics, useful for long-term climate change regulations and policy formulation [21]. Remote sensing techniques offer spatially-explicit spectral information at a larger spatial extent, which is necessary for both local and regional prediction and monitoring of the aboveground carbon stock in reforested areas [18,19]. Recently, new generation commercial sensors such as the WorldView series have been widely used in estimating aboveground carbon stock and biomass [22–24]. These sensors consist of fewer but strategically positioned spectral wavebands, including unique band settings within the red-edge region invaluable for enhancing vegetation spectral response [22,23,25]. However, despite their effectiveness in modelling carbon stocks, they are costly and not readily available. Such limitations hinder frequent quantification and monitoring of aboveground forest carbon stocks in regions such as Southern Africa, where financial constraints limit the availability of spatial data. Hence, improved and freely-available multispectral sensors remain the most feasible sources of spatio-temporal data for predicting forest carbon stock. Specifically, the emergence of cutting-edge freely available multispectral sensors such as the Sentinel-2 offer better prospects for vegetation modelling and monitoring. The sensor is characterised by improved spatial, spectral, and radiometric properties that offer unprecedented opportunities for estimating aboveground carbon stock at both local and regional scales. Sentinel-2 is regarded as an intermediate spatial data source between medium spatial resolution (e.g., Landsat series) and high spatial resolution sensors (e.g., Worldview-2 and RapidEye) due to its strategically positioned band settings in the red-edge region and varying spatial resolution ranging from 10 to 60 m [26,27]. In addition, Sentinel-2 has a higher (five days) temporal resolution, suitable for frequent quantification, monitoring, and management of forest ecosystems and carbon stocks. Despite the recent popularity of Sentinel-2 datasets in vegetation mapping, no study, to the best of our knowledge, has used it to characterise an urban reforested landscape. In addition, new and unique indices derived from red-edge region of Sentinel-2 multispectral image (MSI) for carbon stock estimation in reforested urban landscapes have not been concisely explored. Such indices optimise spectral reflectance that can significantly improve prediction accuracy of terrestrial carbon stock. Studies that have evaluated red-edge indices (e.g., red-edge normalised difference vegetation index, red-edge chlorophyll index and red-edge modified simple ratio index) have particularly focused on leaf area index and biomass estimation [25,28,29].

Thus, there is a need to test such unique indices derived from strategically positioned red-edge bands of Sentinel-2 MSI for enhancing carbon stock estimation in reforested urban landscapes.

Multiple linear regression approaches based on a range of variables are often used for modelling aboveground vegetation biomass and carbon stocks [25,30]. However, optimal prediction of carbon stocks in urban reforested areas requires robust machine learning algorithms that do not have assumptions of data normality. For instance, non-parametric ensemble techniques such as the random forest have proven to be successful in modelling forest ecosystems properties with unprecedented performance [18,25,31]. Random forest is an algorithm known for its bootstrapping and creation of a subset of explanatory variables that are randomly selected from the input dataset, hence overcoming overfitting [22,32]. RF is also capable of addressing complex correlation problems existing between predictor variables due to large volumes of data and noise [33]. Literature shows that the random forest regression model performs better than other machine learning algorithms in vegetation modelling [34–37]. Ghosh and Behera [34] for instance, established that random forest regression model outperforms stochastic gradient boosting in estimating forest aboveground biomass. Similarly, Safari et al. [36] found that random forest model was robust in modelling forest aboveground carbon stock, compared to support vector machine and boosted regression trees. In comparing the performances of random forest, back-propagation neural network, and support vector regression in estimating wetland aboveground biomass, Wan et al. [37] found that random forest performed better than other regression algorithms. However, studies that have utilised random forest to estimate aboveground biomass and carbon content have been restricted to natural and plantation forests. For example, Dube et al. [22] used random forest ensemble to estimate above ground biomass of Eucalyptus and pine species in a commercial forest. Similarly, Odebiri et al. [9] adopted ensemble random forest model to predict soil organic carbon stock in plantation forests, while Mutanga et al. [25] demonstrated that random forest model is critical in predicting biomass in a wetland. Furthermore, it has been widely proven that the integration of Sentinel-2's spectral bands and vegetation indices in a robust machine learning algorithm facilitates accurate determination of aboveground vegetation carbon stocks [26,38–41]. Dang et al. [39] for instance, integrated spectral indices and bands derived from Sentinel-2 MSI in the random forest algorithm to estimate aboveground biomass of forest ecosystems in Yok Don Park, Vietnam. Likewise, Wang et al. [41] used spectral indices derived from Sentinel-2 MSI bands to predict aboveground biomass and leaf area index using robust algorithms such as support vector machine and random forest. The study conducted by Baloloy et al. [38] also indicated that Sentinel-2 derived indices and spectral bands are critical in modelling vegetation metric such as biomass and carbon. In this regard, this study sought to examine the prospect of Sentinel-2 image spectral-data in quantifying carbon stock within a reforested urban landscape.

2. Materials and Methods

2.1. The Study Area

This study was conducted in Buffelsdraai area, North of the Durban city centre in KwaZulu-Natal province, South Africa (Figure 1). Buffelsdraai is a reforested area situated between 30°58'20.08"E and 29°37'55.17"S and covers approximately 800 ha. The area experiences average annual temperatures between 22–27 °C and average annual rainfall ranging from 600–1000 mm. The area is characterized by uneven topography supported by dwyka tillite geological formation [3]. The most dominant reforested tree species in the area are *Acacia* (i.e., *caffra* and *robusta*), *Syzygium cordatum* (water berry), *Bridelia micrantha*, *Dalbergia obovate*, *Erythrina caffra*, and *Silver oak*.

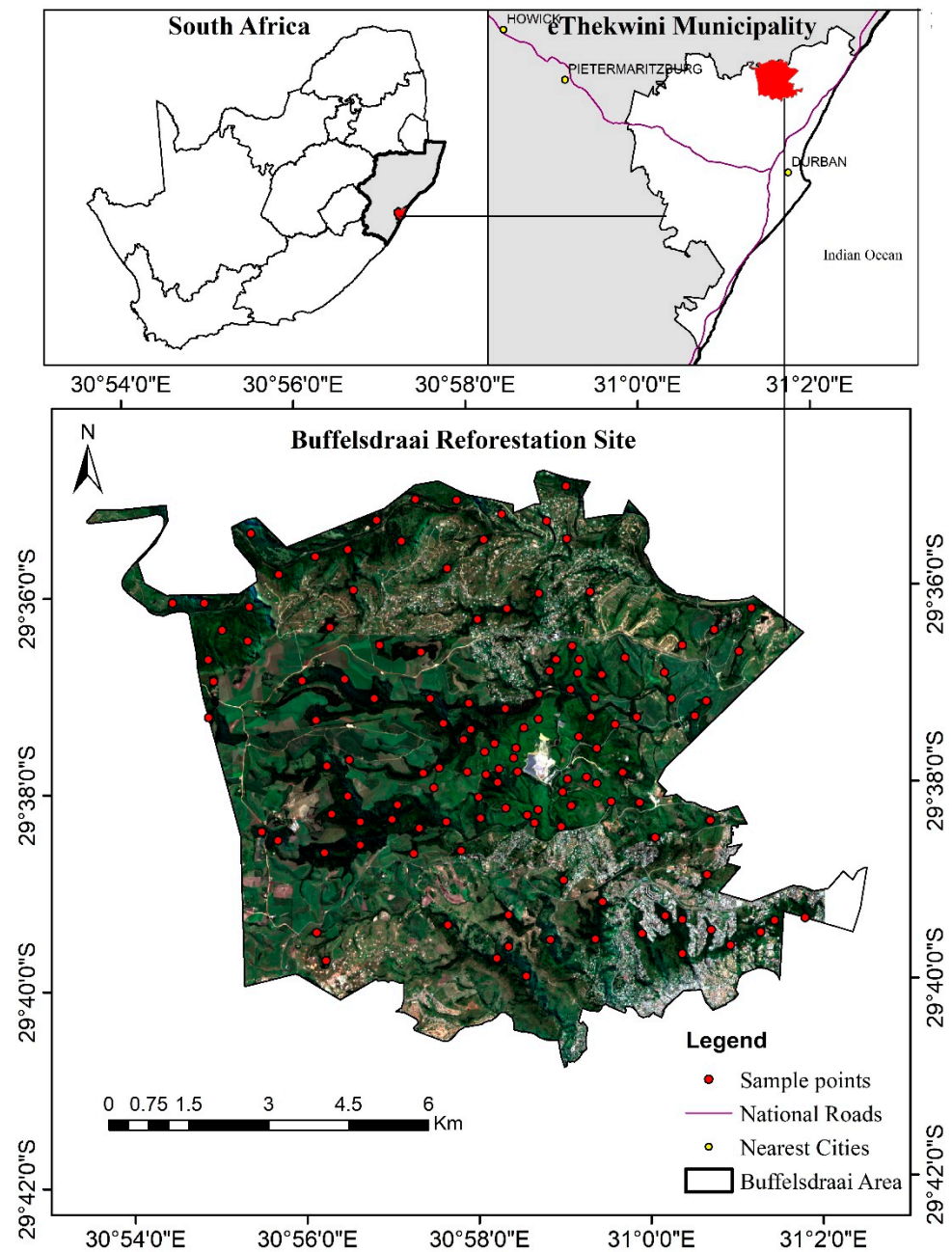


Figure 1. Location of Buffelsdraai reforestation site and sample points, within the eThekweni Municipality in KwaZulu-Natal Province.

2.2. Field-Survey and Data Collection

Field survey and data collection were conducted between 21st and 25th of February 2020 during the summer season at peak biomass productivity. In this study, about 130 pre-determined random sampling points inserted in a global positioning system (GPS) were used to access the sampling sites. From each random point, a plot-size window of 10 m * 10 m was established and structural attributes such as height and diameter at breast height of reforested trees recorded. A clinometer (Vertex IV Hypsometer) was used to measure tree height, while diameter at breast height (DBH) was measured using a calliper. In this study, the Trimble Global Positioning System (GPS) with 0.5 m accuracy was used to record geographic location of each sampled tree.

2.3. Allometric Modelling of Aboveground Biomass and Carbon Stock

The allometric relationship between the tree diameter and height can significantly affect tree biomass, and hence their measurements could be effectively used for vegetation biomass estimation [16,18]. A non-environmental destructive approach such as allometric model for biomass estimation has been recommended by the Intergovernmental Panel on Climate Change (IPCC) [42,43]. In this study, a field measured diameter at breast height (DBH) and height (H) of individual reforested trees were integrated into the allometric model to compute aboveground biomass using the following generic equation:

$$W = a(D^2H)^b$$

where W is the aboveground biomass, D represents diameter at breast height (cm), H indicates tree height (m), while a and b are regression coefficients [42].

Generally, the aboveground dry biomass holds about 50% of carbon, as such, a friction factor of 0.5 is commonly used for converting dry mass into carbon concentration [43,44]. Therefore, in this study, we converted the computed biomass into carbon stock using a factor of 0.5.

2.4. Image Acquisition and Pre-Processing

A multispectral Sentinel-2A satellite image was captured on the 26th of February 2020 during cloud-free day and freely downloaded on the 2nd of March 2020 through the Quantum Geographic Information System (QGIS) portal. Sentinel-2 sensor acquires images at 13 spectral channels (e.g., coastal-b1, blue-b2, green-b3, red-b4, red-edge-b5, red-edge-b6, red-edge-b7, near infrared-b8, red-edge-b8A, water vapour-b9, cloud-b10, shortwave infrared-b11 and shortwave infrared-b12) at varying spatial resolutions of 10, 20, and 60 m. This sensor covers strategically located red-edge region (i.e., b5, 6, 7 and 8A) of the electromagnetic spectrum with unique band settings that are critical for vegetation modelling [26]. Sentinel-2A data is readily available for frequent vegetation assessment and monitoring. In this study, the spectral data was atmospherically corrected using Dark Object Subtraction (DOS) embedded in QGIS software, which also converted spectral radiances to reflectance. Furthermore, the spectral data were extracted from a series of waveband combinations representing vegetation green biomass indices (Table 1). Indices which were ideal for vegetation assessment and monitoring include; normalized difference vegetation index (NDVI), enhanced vegetation index (EVI), green NDVI (GNDVI), transformed vegetation index (TVI1), green chlorophyll index (Cl_{green}), modified simple ratio index (MSRI), ratio vegetation index (RVI), triangular vegetation index (TVI2), advanced vegetation index (AVI), modified triangular vegetation index (MTVI 1 and 2), and normalize pigment chlorophyll ratio index (NPCRI). We also derived indices from a combination of red-edge bands such as the red-edge normalized difference vegetation index ($NDVI_{RE}$), red-edge chlorophyll index (Cl_{RE}), and modified simple ratio red-edge index ($MSRI_{RE}$). In addition, the derived indices were combined with spectral data extracted from the individual bands.

Table 1. Spectral indices derived from Sentinel-2 MSI and their formulae.

Indices	Formulae	References
NDVI	$\frac{NIR - Red}{NIR + Red}$	[45]
EVI	$2.5 * \left(\frac{NIR - Red}{(NIR + 6 * Red - 7.5 * Blue + 1)} \right)$	[46]
TVI1	$\sqrt{(NDVI)} + 0.5$	[47]
GNDVI	$\frac{NIR - Green}{NIR + Green}$	[48]
CI _{green}	$\frac{NIR}{Green} - 1$	[49]
RVI	$\frac{NIR}{Red}$	[50]
MSRI	$\frac{\frac{NIR}{Red} - 1}{\sqrt{\frac{NIR}{Red} + 1}}$	[51]
TVI2	$0.5 * [120 * (NIR - Green) - 200 * (Red - Green)]$	[52]
AVI	$\sqrt[3]{NIR * (1 - Red) * (NIR - Red)}$	[53]
MTVI1	$1.2 * (NIR - Green) - 2.5 * (Red - Green)$	[54]
MTVI2	$\frac{1.5 * (1.2 * (NIR - Green) - 2.5 * (Red - Green))}{\sqrt{(2 * NIR + 1)^2 - (6 * NIR - 5 * \sqrt{(Red)}) - 0.5}}$	[54]
NPCRI	$\frac{Red - Blue}{Red + Blue}$	[55]
NDVI _{RE}	$\frac{NIR - RE}{NIR + RE}$	[29]
CI _{RE}	$\frac{NIR}{RE} - 1$	[49]
MSRI _{RE}	$\frac{\frac{NIR}{RE} - 1}{\sqrt{\frac{NIR}{RE} + 1}}$	[51]

2.5. Statistical Analysis

In this study, random forest algorithm was used for regression analysis. Random forest (RF) operates as an ensemble learning that creates multitude of decision trees (*ntree*) and selects the final best tree based on the majority vote. RF uses a bootstrapping technique to reduce model variance without increasing bias while enhancing accuracy and reducing overfitting [32,56]. Such an ensemble model has a modified technique (e.g., feature bagging) for selecting a random subset of features (*mtry*) in order to determine the split at each tree node [56]. Each node in the model represents a predictor variable and all selected subset of the data are used as response variables. Random forest first examines and tests all predictors from each node before randomly selecting the best split from a set of predictors [22,56]. Furthermore, random forest permits model optimization for better results using two parameters, namely *ntree*, based on large sets of decision trees and bootstrap training sample, and *mtry*, based on the individual predictor variables selected from each tree node [25,40]. Normally, the standard value of *ntree* is set at 500, while *mtry* takes the square-root of the total number of an input predictor variable on a normal classification; on the regression, it divides all predictor variables by a default factor of three [9,56]. The optimal *ntree* and *mtry* values for best prediction performance are determined based on the smallest out-of-bag error [56]. In this study, the *ntree* was adjusted between 100 and 500 at the interval value of 100, whereas *mtry* was adjusted from 1 to 25 with interval value of 1. The best *ntree* and *mtry* was determined at the interval value of 300 and 18 based on the least root mean square error of the training dataset (n = 56).

2.6. Optimal Predictor Variables Selection

Commonly, regression analysis suffers a problem of multi-collinearity due to high correlation or less variability between some input predictor variables [9,40]. Despite the capability of an ensemble method such as random forest in dealing with strong correlation between certain variables, it is necessary to select and utilize optimal predictor variables which improve regression model performance. In this study, the out-of-bag (OOB) approach based on backward elimination was used to determine a subset of predictor variables that were ideal for the best regression model. Backward elimination is critical for removing highly correlated variables, which are not important until a subset of ideal predictor variables remain in the model. In addition, the values of carbon stock estimated from a subset of predictor variables were used to generate a spatially varying map of carbon stock.

2.7. Model Validation and Accuracy Assessment

Random forest effectiveness in predicting carbon stock within the urban landscape was tested using 10-fold cross-validation. Initially, the total dataset ($n = 80$) was partitioned into 70% ($n = 56$) as training sets and 30% ($n = 24$) as testing datasets. The RF model performance was evaluated using the coefficient of determination (R^2), root mean square error (RMSE) and mean absolute Error (MAE).

3. Results

3.1. Carbon Stock of Reforested Trees

Based on the descriptive statistics, the minimum and maximum value of measured carbon stock within reforested urban landscape are 0.244 and 10.20 $\text{t}\cdot\text{ha}^{-1}$ with the mean value of 3.386 $\text{t}\cdot\text{ha}^{-1}$ and standard deviation of 2.475 $\text{t}\cdot\text{ha}^{-1}$.

3.2. Random Forest Model Optimization

Figure 2 shows random forest optimization parameters ($Ntree$ and $Mtry$). In this study, the $Ntree$ value of 300 and $Mtry$ value of 18 produced the lowest RMSE (0.125 $\text{t}\cdot\text{ha}^{-1}$) and were selected for further carbon stock prediction.

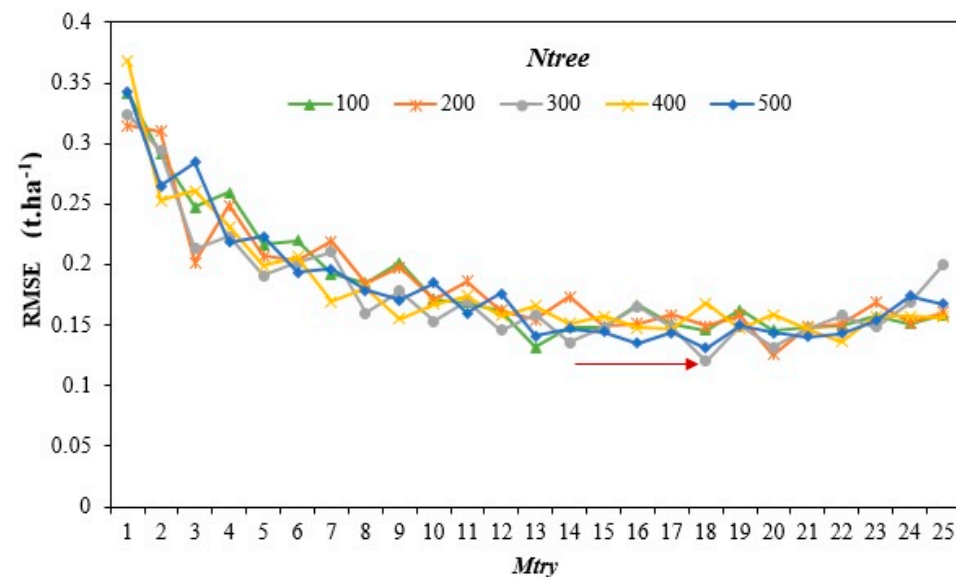


Figure 2. Best random forest optimization parameters ($Ntree$ and $Mtry$) selected based on the lowest RMSE indicated by the red arrow.

3.3. Variable Importance Selection

Results in Figure 3 show the predictive performance of individual variables used in the model and their ranking in terms of importance based on the OOB error rate, which increases with importance, while Figure 4 illustrates the number of variables selected for optimal carbon stock prediction. Using the backward elimination approach, a subset of four predictor variables (i.e., NDVI, EVI, MSRI and NDVI_{RE}) with the smallest error rate was selected for the final carbon stock model. The integration of this subset into one random forest model produced the lowest OOB RMSE of 0.143 $\text{t}\cdot\text{ha}^{-1}$ and a 10-fold cross-validation RMSE of 0.153 $\text{t}\cdot\text{ha}^{-1}$. The RMSE increased to 0.331 $\text{t}\cdot\text{ha}^{-1}$ and 0.345 $\text{t}\cdot\text{ha}^{-1}$ for both OOB and 10-fold cross validation when using all 25 variables in the training dataset. Finally, this study used four predictor variables (i.e., NDVI, EVI, MSRI, and NDVI_{RE}) in the final random forest regression model for predicting carbon stock within the study area.

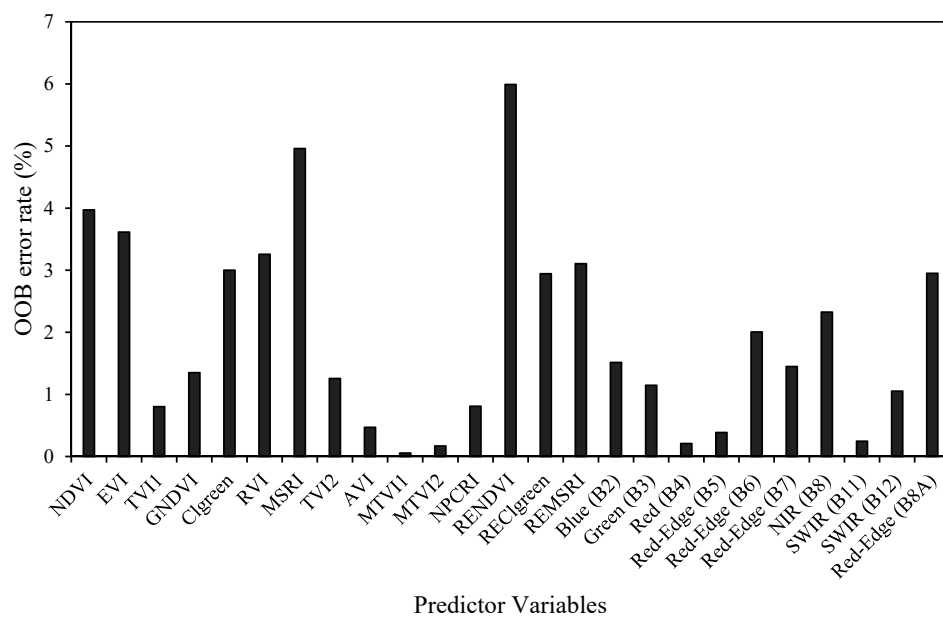


Figure 3. The importance of variables in predicting carbon stock using the random forest model. The mean increase in OOB error rate shows greater variable significance.

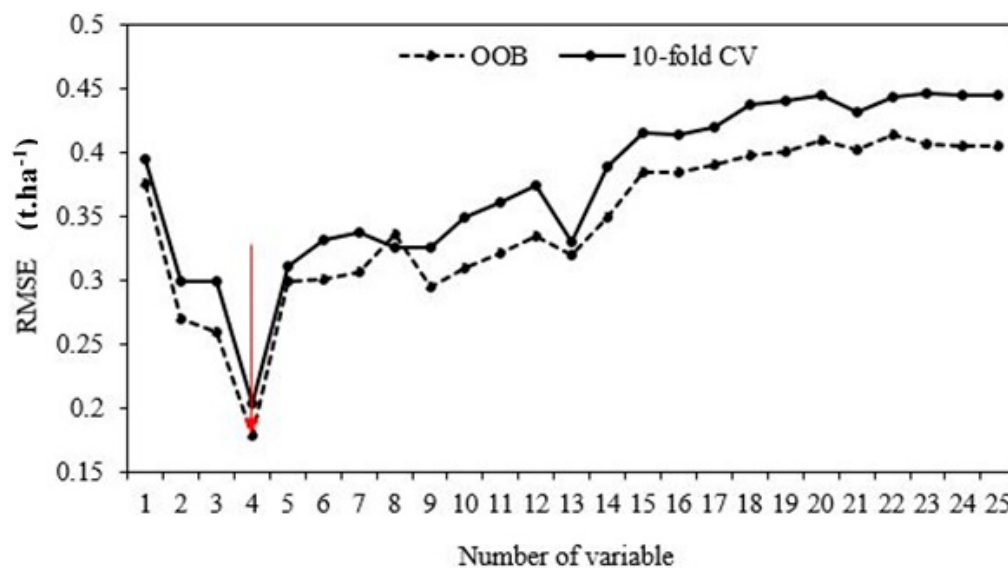


Figure 4. Selection of optimal number of predictor variables using backward elimination approach. The ideal number of variables (indicated with red arrow) was selected based on the RMSE generated from the training dataset using OOB and 10-fold cross validation.

3.4. Random Forest Model Prediction Performance

Results in Table 2 show the overall mean carbon stock and prediction performance of Sentinel-2's spectral data and the random forest model. The integration of optimal variables selected by random forest produced an overall mean carbon stock of 3.389 and 3.642 t·ha⁻¹ using calibration (training) and validation (testing) datasets. The random forest regression model obtained highest R² (from 77.96 to 79.82%) with lowest RMSE (from 0.378 to 0.466 t·ha⁻¹) and MAE (from 0.189 to 0.233 t·ha⁻¹) when predicting carbon stock using four selected indices combined together, compared to the use of individual indices into the model. Figure 5 illustrates the relationship between predicted carbon stock with allometric derived carbon stock and optimal variables that greatly improved the random forest prediction model. Results in Figure 5 also show a strong correlation coefficient (r)

of 0.951 to 0.978 between predicted and measured carbon stock. Furthermore, Figure 6 represent spatial variability of carbon stock across reforested urban landscape. Generally, the spatial variability of carbon stock increases with increasing canopy cover and decreases with the decrease in green biomass.

Table 2. Performance of random forest model in predicting reforested carbon stock using selected subset of variables separated into calibration and validation datasets.

Prediction Dataset	Mean C (t·ha ⁻¹)	R ² (%)	RMSE (t·ha ⁻¹)	MAE (t·h ⁻¹)
Calibration	3.389	79.82	0.378 (11.15%)	0.189
Validation	3.642	77.96	0.466 (12.79%)	0.233

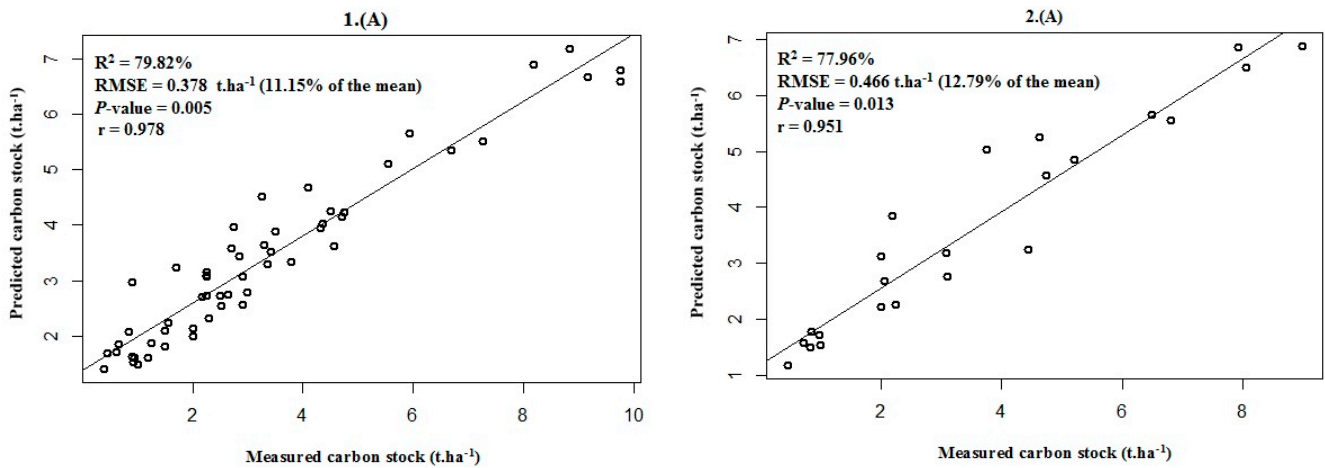


Figure 5. Relationship between predicted and measured carbon stock of reforested urban landscape for calibration (1) and validation (2) datasets. The regression analysis between predicted and measured carbon stock was established using a combined subset of optimal indices (A).

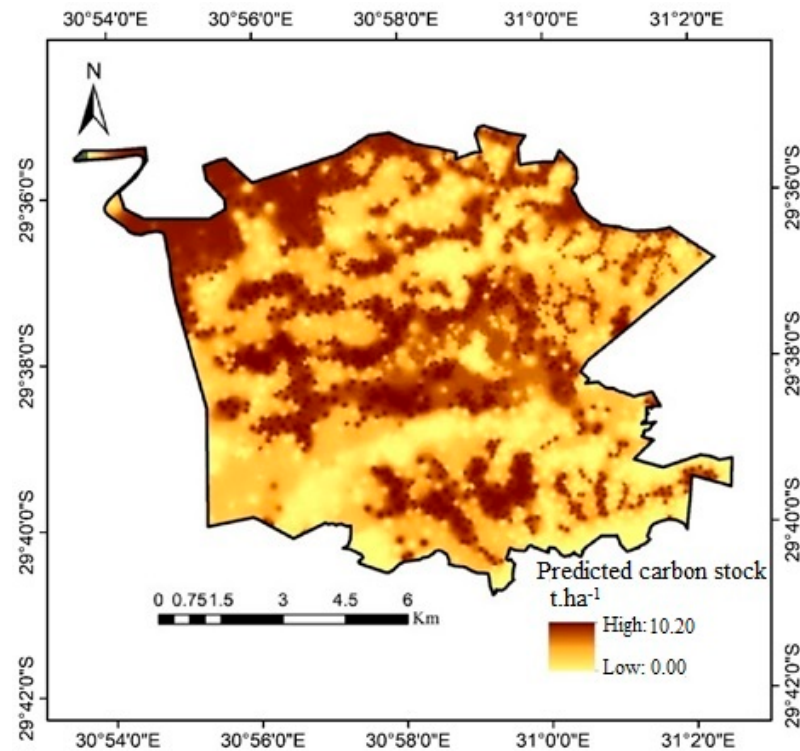


Figure 6. Prediction map of carbon stock within reforested urban landscape using random forest model.

4. Discussion

Concise estimation of climate regulating ecosystem services provided by reforested urban trees such as carbon stock is key to understanding the role and value of reforestation strategy in the global carbon dynamics and climate change regulation potential. Hence, this study sought to test the utility of Sentinel-2 satellite data in quantitatively evaluating the amount of carbon in an urban reforested landscape.

Results showed that Sentinel-2 spectral data could be used to estimate carbon stocks in an urban reforested area. In this study, a mean carbon stock of between 3.389 and 3.642 t·ha⁻¹, with high R² (77.96 and 79.82%), low RMSE (0.378 and 0.466 t·ha⁻¹), and MAE (0.189 and 0.233) was obtained using calibration and validation subsets dataset. This reasonable estimation performance can be explained by Sentinel-2's strategically positioned wavebands, particularly the red-edge region. The region records numerous leaf properties such as chlorophyll concentration, leaf area index and green-biomass, necessary for measuring forests services such biomass and carbon stock [21,22,57]. Hence, its inclusion as an explanatory variable significantly improved carbon stock modelling accuracy. Our results concur with the hypothesis that sensors (e.g., Sentinel-2 MSI) with strategically located band settings such as red-edge, offer unprecedented spectral information critical for measuring vegetation metrics and services such as biomass and carbon uptake [22,25]. In addition to the red-edge, Sentinel-2's near infrared (NIR) bands also provide sensitive spectral reflectance capable of explicit estimation of vegetation metrics such as biomass and carbon stock. The near-infrared region offers a refined narrow spectral wavelength ranging between 850 and 880 nm and highly sensitive to the biophysical and biochemical response of vegetation [20,58]. Biophysical (e.g., leaf area, biomass) and biochemical (e.g., chlorophyll content) properties are critical for detecting vegetation health and productivity (useful for determining carbon uptake by reforested trees).

Results of this study also showed a strong correlation (r : 0.95 to 0.98) between the estimated aboveground carbon stock and measured carbon stock using calibration and validation datasets. Such a strong relationship is associated with the consolidation of optimal variables (i.e., NDVI, EVI, MSRI, and NDVI_{RE}) selected by backward elimination process for the final prediction model of carbon stock. Among the integrated vegetation indices, NDVI was valuable in the estimation of carbon stock within reforested urban landscape. This could be attributed to the fact that NDVI is an important indicator of green-biomass, which can be effectively used for deriving and monitoring spatio-temporal dynamics of aboveground carbon stock/sequestration [59–61]. The findings in this study are consistent with those of Moumouni et al. [61] who predicted aboveground carbon stock variability across different forest biomes to a R² of 0.91 using an NDVI. Meanwhile, in a related study, Bindu et al. [59] attained an R² of 0.71 in estimating carbon stock of mangroves trees using NDVI. Such a strong predictive performance of NDVI in carbon stock estimation can be explained by the sensitivity of the near-infrared region to the internal leaf mesophyll, which is a major indicator of vegetation health and is responsible for maximum biomass productivity [62,63], and hence critical for simulating the amount of carbon stored in forest ecosystems. NDVI contain robust spectral information derived from Red and NIR bands, which are sensitive in detecting vegetation health and productivity, which are valuable carbon accumulation indicators. According to Moumouni et al. [61], the spatio-temporal variability in green-biomass reflectance as measured by NDVI is proportional to the simulated carbon flux. Interestingly, the inclusion of new and unique red-edge indices such as NDVI_{RE} boosted the predictive performance of carbon stock within reforested urban landscape. The robustness of red-edge indices (i.e., NDVI_{RE}) lies with the ability to provide spectral reflectance that have less atmospheric, soil background and water absorption influence or effects [25,29]. The findings in this study are congruous with previous studies, which also established that red-edge indices are highly sensitive to vegetation metrics (e.g., leaf area index and biomass) [25,28,29,64]. For instance, Xie et al. [64] found that the red-edge derived spectral indices are better prospects for improving estimation coefficient of leaf area index in agroecosystems. While Mutanga et al. [25] established that

red-edge indices can significantly increase biomass estimation of wetland vegetation. These studies suggested that red-edge indices could be effectively used to measure vegetation productivity and health (which includes carbon sequestration and stock). Red-edge derived indices are less prone to saturation that is common to standard NDVI [28,29], and hence can be effectively applied in dense vegetation cover. In addition, red-edge indices contain sensitive spectral data as red-edge wavebands record rapid variations in plants chlorophyll content and leaf structure, hence critical for monitoring the spatial and temporal dynamics of vegetation health and productivity [65,66]. Furthermore, the results on the carbon stock map show the variability of carbon stock across the study area, which decreases with the decrease in canopy density. This variability in carbon stock within the study area can be attributed to the variations in landscape topographic characteristics, which influence vegetation density and productivity. For example, studies have shown that slope, elevation and aspect can significantly affect the spatial distribution of carbon stock across forest landscapes [9,67,68]. Variations can also be triggered by forest species composition due to the differences in biophysical (i.e., leaf area, stomata and canopy structure) and biochemical (i.e., leaf pigments, lignin, and carotenoids) characteristics [69–71]. For instance, deciduous trees (e.g., *Acacia* and *Dalbergia*) consist of large leaf stomatal properties which increase plant productivity and carbon storage, whereas shrub trees such as *Artemisia* have limited structural geometry, stem, and leaf biomass, thereby contributing to low carbon stock [72,73].

In addition, the application of robust regression models such as random forest significantly improved the prediction performance of carbon stock in the reforested urban landscape. The robustness of the random forest algorithm is associated with the ability to select important variables required for the best regression model [9,25]. For instance, the consolidation of NDVI, EVI, MSRI, and NDVI_{RE} derived from Sentinel-2 MSI as selected by random forest model offers a remarkable methodology for predicting carbon stock in a reforested urban landscape. Overall, this study presents a better and cost-effective option for quantifying carbon stock in the reforested urban landscape using freely and readily available new generation Sentinel-2 MSI. Moreover, the study demonstrates the significance of the reforestation initiative in reducing atmospheric carbon emissions and regulating climate systems within the urban landscape, hence suggesting effective management and monitoring practices for reforested ecosystems and their services. The information presented in this study is useful for planning large-scale reforestation projects in order to maximize sequestration capacity and improve climate change regulation potential within urban landscapes. Our approach presents a concise methodology to monitor the progress of urban reforestation projects locally and similar reforestation projects around the world. In addition, although these results may benefit forest managers and decision makers, multi-temporal information on aboveground carbon stock variability across seasons and years and effect of topography on carbon sequestration within reforested urban areas still requires investigation. Furthermore, the inaccessibility of high spatial resolution images (e.g., Worldview-3, Quickbird etc.) and associated costs limited the opportunity to estimate carbon stock at a species level.

5. Conclusions

This study sought to examine the prospect of Sentinel-2 image spectral-data for predicting carbon stock in the reforested urban landscape. Based on the findings it is concluded that:

- The spectral information derived from Sentinel-2 MSI can be effectively used to model or predict climate regulating ecosystem services such as carbon stock in reforested urban landscape.
- Spectral indices (e.g., NDVI, EVI, MSRI, and NDVI_{RE}) are useful in enhancing prediction performance of carbon stock in reforested urban environment.

The findings of this study are critical for understanding the contribution of reforestation strategy in the global carbon balance and climate change regulation potential as

required by Kyoto-Protocol and Reducing Emissions from Deforestation and Forest Degradation (REDD+). The study also provides information that is beneficial to decision-and policy-makers and forest managers to design optimal management policies and increase reforestation projects. Also, the study demonstrates the significance of the reforestation initiative in reducing atmospheric carbon emissions and regulating climate systems within the urban landscape, hence can be used to suggest effective management and monitoring practices for reforested ecosystems and their services. Overall, we conclude that Sentinel-2 spectral information can be effectively used for predicting and monitoring carbon flux in the reforested urban landscape. Furthermore, dataset and approaches adopted in this study are easily transferable to similar initiatives globally due to S-2's free availability and global coverable. Also, the random forest ensemble has been proven to be robust in estimating forest carbon.

Author Contributions: M.M.: Developed the aim and objective of the research including conceptualization of manuscript. Among other things, contributed to collection of field measurements and analysis of dataset, as well as the write-up of the initial manuscript draft including. J.O. as the main supervisor, verified the analytical approaches and results of the study including interpretation and discussion of the obtained results. Provided constructive criticism and comments which improved our manuscript. O.M. as the co-supervisor, sharpened the novelty of aim and objective, including the smoothness of the entire manuscript, especially the introduction, type of data used and discussion. All authors have read and agreed to the published version of the manuscript.

Funding: This research received no external funding.

Institutional Review Board Statement: Not applicable.

Informed Consent Statement: Not applicable.

Data Availability Statement: Data availability is restricted for security or ethical reasons involving ongoing research project.

Acknowledgments: The authors would like to acknowledge the DST-NRF SARCHI Chair in Land Use Planning and Management at UKZN (Grant No. 84157) for their financial support. A special acknowledgement to Durban municipality through the Durban Research Action Partnership (DRAP) for allowing this research project to be carried out on their protected reforestation site.6. We further thank the reviewers for their constructive criticism which improved this research work.

Conflicts of Interest: The authors declare no conflict of interest.

References

1. Adamu, B.; Rasul, A.; Whanda, S.J.; Headboy, P.; Muhammed, I.; Maiha, I.A. Evaluating the accuracy of spectral indices from Sentinel-2 data for estimating forest biomass in urban areas of the tropical savanna. *Remote Sens. Appl. Soc. Environ.* **2021**, *22*, 100484.
2. Odindi, J.; Mhangara, P. Green spaces trends in the city of Port Elizabeth from 1990 to 2000 using remote sensing. *Int. J. Environ. Res.* **2012**, *6*, 653–662.
3. Sithole, K.; Odindi, J.; Mutanga, O. Assessing the utility of topographic variables in predicting structural complexity of tree stands in a reforested urban landscape. *Urban For. Urban Green.* **2018**, *31*, 120–129. [[CrossRef](#)]
4. Livesley, S.; McPherson, E.; Calfapietra, C. The urban forest and ecosystem services: Impacts on urban water, heat, and pollution cycles at the tree, street, and city scale. *J. Environ. Qual.* **2016**, *45*, 119–124. [[CrossRef](#)]
5. Xu, G.; Jiao, L.; Zhao, S.; Yuan, M.; Li, X.; Han, Y.; Zhang, B.; Dong, T. Examining the impacts of land use on air quality from a spatio-temporal perspective in Wuhan, China. *Atmosphere* **2016**, *7*, 62. [[CrossRef](#)]
6. Luederitz, C.; Brink, E.; Gralla, F.; Hermelingmeier, V.; Meyer, M.; Niven, L.; Panzer, L.; Partelow, S.; Rau, A.-L.; Sasaki, R.; et al. A review of urban ecosystem services: Six key challenges for future research. *Ecosyst. Serv.* **2015**, *14*, 98–112. [[CrossRef](#)]
7. Cho, M.A.; Debba, P.; Mutanga, O.; Dudeni-Tlhone, N.; Magadla, T.; Khuluse, S.A. Potential utility of the spectral red-edge region of SumbandilaSat imagery for assessing indigenous forest structure and health. *Int. J. Appl. Earth Obs. Geoinf.* **2012**, *16*, 85–93. [[CrossRef](#)]
8. Keenan, R.J.; Reams, G.A.; Achard, F.; de Freitas, J.V.; Grainger, A.; Lindquist, E. Dynamics of global forest area: Results from the FAO Global Forest Resources Assessment 2015. *For. Ecol. Manag.* **2015**, *352*, 9–20. [[CrossRef](#)]
9. Odebiri, O.; Mutanga, O.; Odindi, J.; Peerbhay, K.; Dovey, S. Predicting soil organic carbon stocks under commercial forest plantations in KwaZulu-Natal province, South Africa using remotely sensed data. *GIScience Remote Sens.* **2020**, *57*, 450–463. [[CrossRef](#)]

10. Payn, T.; Carnus, J.-M.; Freer-Smith, P.; Kimberley, M.; Kollert, W.; Liu, S.; Orazio, C.; Rodriguez, L.; Silva, L.N.; Wingfield, M.J. Changes in planted forests and future global implications. *For. Ecol. Manag.* **2015**, *352*, 57–67. [[CrossRef](#)]
11. Mundia, C.N.; Aniya, M. Analysis of land use/cover changes and urban expansion of Nairobi city using remote sensing and GIS. *Int. J. Remote Sens.* **2005**, *26*, 2831–2849. [[CrossRef](#)]
12. Pellikka, P.; Heikinheimo, V.; Hietanen, J.; Schäfer, E.; Siljander, M.; Heiskanen, J. Impact of land cover change on aboveground carbon stocks in Afromontane landscape in Kenya. *Appl. Geogr.* **2018**, *94*, 178–189. [[CrossRef](#)]
13. Curiel-Esparza, J.; Gonzalez-Utrillas, N.; Canto-Perello, J.; Martin-Utrillas, M. Integrating climate change criteria in reforestation projects using a hybrid decision-support system. *Environ. Res. Lett.* **2015**, *10*, 094022. [[CrossRef](#)]
14. Deo, R.K.; Russell, M.B.; Domke, G.M.; Andersen, H.-E.; Cohen, W.B.; Woodall, C.W. Evaluating site-specific and generic spatial models of aboveground forest biomass based on Landsat time-series and LiDAR strip samples in the Eastern USA. *Remote Sens.* **2017**, *9*, 598. [[CrossRef](#)]
15. Baccini, A.; Laporte, N.; Goetz, S.; Sun, M.; Dong, H. A first map of tropical Africa's above-ground biomass derived from satellite imagery. *Environ. Res. Lett.* **2008**, *3*, 045011. [[CrossRef](#)]
16. Dube, T.; Mutanga, O. Evaluating the utility of the medium-spatial resolution Landsat 8 multispectral sensor in quantifying aboveground biomass in uMgeni catchment, South Africa. *ISPRS J. Photogramm. Remote Sens.* **2015**, *101*, 36–46. [[CrossRef](#)]
17. Henry, M.; Picard, N.; Trotta, C.; Manlay, R.; Valentini, R.; Bernoux, M.; Saint-André, L. Estimating tree biomass of sub-Saharan African forests: A review of available allometric equations. *Silva Fenn.* **2011**, *45*, 477–569. [[CrossRef](#)]
18. Dube, T.; Mutanga, O. Quantifying the variability and allocation patterns of aboveground carbon stocks across plantation forest types, structural attributes and age in sub-tropical coastal region of KwaZulu Natal, South Africa using remote sensing. *Appl. Geogr.* **2015**, *64*, 55–65. [[CrossRef](#)]
19. Hickey, S.; Callow, N.J.; Phinn, S.; Lovelock, C.; Duarte, C.M. Spatial complexities in aboveground carbon stocks of a semi-arid mangrove community: A remote sensing height-biomass-carbon approach. *Estuar. Coast. Shelf Sci.* **2018**, *200*, 194–201. [[CrossRef](#)]
20. Matongera, T.N.; Mutanga, O.; Dube, T.; Sibanda, M. Detection and mapping the spatial distribution of bracken fern weeds using the Landsat 8 OLI new generation sensor. *Int. J. Appl. Earth Obs. Geoinf.* **2017**, *57*, 93–103. [[CrossRef](#)]
21. Gara, T.W.; Murwira, A.; Ndaimani, H. Predicting forest carbon stocks from high resolution satellite data in dry forests of Zimbabwe: Exploring the effect of the red-edge band in forest carbon stocks estimation. *Geocarto Int.* **2016**, *31*, 176–192. [[CrossRef](#)]
22. Dube, T.; Mutanga, O.; Elhadi, A.; Ismail, R. Intra-and-inter species biomass prediction in a plantation forest: Testing the utility of high spatial resolution spaceborne multispectral rapideye sensor and advanced machine learning algorithms. *Sensors* **2014**, *14*, 15348–15370. [[CrossRef](#)]
23. Eckert, S. Improved forest biomass and carbon estimations using texture measures from WorldView-2 satellite data. *Remote Sens.* **2012**, *4*, 810–829. [[CrossRef](#)]
24. Karna, Y.K. Mapping above Ground Carbon Using Worldview Satellite Image and Lidar data In Relationship with Tree Diversity of Forests. Master's Thesis, University of Twente, Twente, The Netherlands, 2012.
25. Mutanga, O.; Adam, E.; Cho, M.A. High density biomass estimation for wetland vegetation using WorldView-2 imagery and random forest regression algorithm. *Int. J. Appl. Earth Obs. Geoinf.* **2012**, *18*, 399–406. [[CrossRef](#)]
26. Korhonen, L.; Hadi; Packalen, P.; Rautiainen, M. Comparison of Sentinel-2 and Landsat 8 in the estimation of boreal forest canopy cover and leaf area index. *Remote Sens. Environ.* **2017**, *195*, 259–274. [[CrossRef](#)]
27. Thanh Noi, P.; Kappas, M. Comparison of random forest, k-nearest neighbor, and support vector machine classifiers for land cover classification using Sentinel-2 imagery. *Sensors* **2018**, *18*, 18. [[CrossRef](#)]
28. Delegido, J.; Verrelst, J.; Meza, C.; Rivera, J.; Alonso, L.; Moreno, J. A red-edge spectral index for remote sensing estimation of green LAI over agroecosystems. *Eur. J. Agron.* **2013**, *46*, 42–52. [[CrossRef](#)]
29. Dong, T.; Liu, J.; Shang, J.; Qian, B.; Ma, B.; Kovacs, J.M.; Walters, D.; Jiao, X.; Geng, X.; Shi, Y. Assessment of red-edge vegetation indices for crop leaf area index estimation. *Remote Sens. Environ.* **2019**, *222*, 133–143. [[CrossRef](#)]
30. Lu, D. The potential and challenge of remote sensing-based biomass estimation. *Int. J. Remote Sens.* **2006**, *27*, 1297–1328. [[CrossRef](#)]
31. Grimm, R.; Behrens, T.; Märker, M.; Elsenbeer, H. Soil organic carbon concentrations and stocks on Barro Colorado Island—Digital soil mapping using Random Forests analysis. *Geoderma* **2008**, *146*, 102–113. [[CrossRef](#)]
32. Ließ, M.; Schmidt, J.; Glaser, B. Improving the spatial prediction of soil organic carbon stocks in a complex tropical mountain landscape by methodological specifications in machine learning approaches. *PLoS ONE* **2016**, *11*, e0153673. [[CrossRef](#)] [[PubMed](#)]
33. Vincenzi, S.; Zucchetta, M.; Franzoi, P.; Pellizzato, M.; Pranovi, F.; de Leo, G.A.; Torricelli, P. Application of a Random Forest algorithm to predict spatial distribution of the potential yield of *Ruditapes philippinarum* in the Venice lagoon, Italy. *Ecol. Model.* **2011**, *222*, 1471–1478. [[CrossRef](#)]
34. Ghosh, S.M.; Behera, M.D. Aboveground biomass estimation using multi-sensor data synergy and machine learning algorithms in a dense tropical forest. *Appl. Geogr.* **2018**, *96*, 29–40. [[CrossRef](#)]
35. Roy, B. Optimum machine learning algorithm selection for forecasting vegetation indices: MODIS NDVI, EVI. *Remote Sens. Appl. Soc. Environ.* **2021**, *23*, 100582.
36. Safari, A.; Sohrabi, H.; Powell, S.; Shataee, S. A comparative assessment of multi-temporal Landsat 8 and machine learning algorithms for estimating aboveground carbon stock in coppice oak forests. *Int. J. Remote Sens.* **2017**, *38*, 6407–6432. [[CrossRef](#)]
37. Wan, R.; Wang, P.; Wang, X.; Yao, X.; Dai, X. Modeling wetland aboveground biomass in the Poyang Lake National Nature Reserve using machine learning algorithms and Landsat-8 imagery. *J. Appl. Remote Sens.* **2018**, *12*, 046029. [[CrossRef](#)]

38. Baloloy, A.B.; Blanco, A.C.; Candido, C.G.; Argamosa, R.J.L.; Dumalag, J.B.L.C.; Dimapilis, L.L.C.; Paringit, E.C. Estimation of mangrove forest aboveground biomass using multispectral bands, vegetation indices and biophysical variables derived from optical satellite imageries: Rapideye, planetscope and sentinel-2. *ISPRS Ann. Photogramm. Remote Sens. Spat. Inf. Sci.* **2018**, *4*, 29–36. [[CrossRef](#)]
39. Dang, A.T.N.; Nandy, S.; Srinet, R.; Luong, N.V.; Ghosh, S.; Kumar, A.S. Forest aboveground biomass estimation using machine learning regression algorithm in Yok Don National Park, Vietnam. *Ecol. Inform.* **2019**, *50*, 24–32. [[CrossRef](#)]
40. Forkuor, G.; Dimobe, K.; Serme, I.; Tondoh, J.E. Landsat-8 vs. Sentinel-2: Examining the added value of sentinel-2's red-edge bands to land-use and land-cover mapping in Burkina Faso. *GIScience Remote Sens.* **2018**, *55*, 331–354. [[CrossRef](#)]
41. Wang, J.; Xiao, X.; Bajgain, R.; Starks, P.; Steiner, J.; Doughty, R.B.; Chang, Q. Estimating leaf area index and aboveground biomass of grazing pastures using Sentinel-1, Sentinel-2 and Landsat images. *ISPRS J. Photogramm. Remote Sens.* **2019**, *154*, 189–201. [[CrossRef](#)]
42. Clark, A., III; Saucier, J.R.; McNab, W.H. *Total-Tree Weight, Stem Weight, and Volume Tables for Hardwood Species in The Southeast*; Georgia Forest Research Paper; Georgia Forest Research: Macon, GA, USA, 1986.
43. Tooichi, E. Carbon sequestration: How much can forestry sequester CO₂. *For. Res. Eng. Int. J.* **2018**, *2*, 148–150. [[CrossRef](#)]
44. Birdsey, R.A. *Carbon Storage and Accumulation in United States Forest Ecosystems*; US Department of Agriculture, Forest Service: Washington, DC, USA, 1992.
45. Rousel, J.; Haas, R.; Schell, J.; Deering, D. Monitoring vegetation systems in the great plains with ERTS. In *Proceedings of the Third Earth Resources Technology Satellite—1 Symposium*; NASA SP-351; NASA: Washinton, DC, USA, 1973.
46. Huete, A.; Justice, C.; van Leeuwen, W. MODIS Vegetation Index (MOD13). *Algorithm Theor. Basis Doc.* **1999**, *3*, 295–309.
47. Deering, D. Measuring “forage production” of grazing units from Landsat MSS data. In *Proceedings of the Tenth International Symposium of Remote Sensing of the Environment*, Ann Arbor, MI, USA, 6 October 1975; pp. 1169–1198.
48. Gitelson, A.A.; Merzlyak, M.N. Remote sensing of chlorophyll concentration in higher plant leaves. *Adv. Space Res.* **1998**, *22*, 689–692. [[CrossRef](#)]
49. Gitelson, A.A.; Gritz, Y.; Merzlyak, M.N. Relationships between leaf chlorophyll content and spectral reflectance and algorithms for non-destructive chlorophyll assessment in higher plant leaves. *J. Plant Physiol.* **2003**, *160*, 271–282. [[CrossRef](#)] [[PubMed](#)]
50. Baret, F.; Guyot, G. Potentials and limits of vegetation indices for LAI and APAR assessment. *Remote Sens. Environ.* **1991**, *35*, 161–173. [[CrossRef](#)]
51. Wu, C.; Niu, Z.; Tang, Q.; Huang, W. Estimating chlorophyll content from hyperspectral vegetation indices: Modeling and validation. *Agric. For. Meteorol.* **2008**, *148*, 1230–1241. [[CrossRef](#)]
52. Broge, N.H.; Leblanc, E. Comparing prediction power and stability of broadband and hyperspectral vegetation indices for estimation of green leaf area index and canopy chlorophyll density. *Remote Sens. Environ.* **2001**, *76*, 156–172. [[CrossRef](#)]
53. Plummer, S. The Angular Vegetation Index: An atmospherically resistant index for the second along track scanning radiometer (ATSR-2). In *Proceedings of the Sixth International Symposium Physical Measurements and Signatures in Remote Sensing*, Val d'Isere, France, 17–21 January 1994.
54. Haboudane, D.; Miller, J.R.; Pattey, E.; Zarco-Tejada, P.J.; Strachan, I.B. Hyperspectral vegetation indices and novel algorithms for predicting green LAI of crop canopies: Modeling and validation in the context of precision agriculture. *Remote Sens. Environ.* **2004**, *90*, 337–352. [[CrossRef](#)]
55. Peñuelas, J.; Gamon, J.; Fredeen, A.; Merino, J.; Field, C. Reflectance indices associated with physiological changes in nitrogen-and water-limited sunflower leaves. *Remote Sens. Environ.* **1994**, *48*, 135–146. [[CrossRef](#)]
56. Breiman, L. Random forests. *Mach. Learn.* **2001**, *45*, 5–32. [[CrossRef](#)]
57. Sibanda, M.; Mutanga, O.; Rouget, M. Comparing the spectral settings of the new generation broad and narrow band sensors in estimating biomass of native grasses grown under different management practices. *GIScience Remote Sens.* **2016**, *53*, 614–633. [[CrossRef](#)]
58. Jia, X.; Chen, S.; Yang, Y.; Zhou, L.; Yu, W.; Shi, Z. Organic carbon prediction in soil cores using VNIR and MIR techniques in an alpine landscape. *Sci. Rep.* **2017**, *7*, 2144. [[CrossRef](#)] [[PubMed](#)]
59. Bindu, G.; Rajan, P.; Jishnu, E.; Joseph, K.A. Carbon stock assessment of mangroves using remote sensing and geographic information system. *Egypt. J. Remote Sens. Space Sci.* **2020**, *23*, 1–9. [[CrossRef](#)]
60. Gizachew, B.; Solberg, S.; Næsset, E.; Gobakken, T.; Bollandsås, O.M.; Breidenbach, J.; Zahabu, E.; Mauya, E.W. Mapping and estimating the total living biomass and carbon in low-biomass woodlands using Landsat 8 CDR data. *Carbon Balance Manag.* **2016**, *11*, 13. [[CrossRef](#)]
61. Moumouni, Y.I.; Zakari, S.; Thomas, O.; Imorou, I.T.; Djaouga, M.; Arouna, O. Mapping of Wood Carbon Stocks in the Classified Forest of Wari-Marou in Benin Center (West Africa). *Int. J. For. Anim. Fish. Res.* **2018**, *2*, 64–73. [[CrossRef](#)]
62. Rafique, R.; Zhao, F.; de Jong, R.; Zeng, N.; Asrar, G.R. Global and regional variability and change in terrestrial ecosystems net primary production and NDVI: A model-data comparison. *Remote Sens.* **2016**, *8*, 177. [[CrossRef](#)]
63. Wang, J.; Rich, P.; Price, K.; Kettle, W. Relations between NDVI and tree productivity in the central Great Plains. *Int. J. Remote Sens.* **2004**, *25*, 3127–3138. [[CrossRef](#)]
64. Xie, Q.; Dash, J.; Huang, W.; Peng, D.; Qin, Q.; Mortimer, H.; Casa, R.; Pignatti, S.; Laneve, G.; Pascucci, S. Vegetation indices combining the red and red-edge spectral information for leaf area index retrieval. *IEEE J. Sel. Top. Appl. Earth Obs. Remote Sens.* **2018**, *11*, 1482–1493. [[CrossRef](#)]

65. Kim, H.-O.; Yeom, J. Benefits of Red-Edge Spectral Band and Texture Features for the Object-Based Classification Using RapidEye Satellite Image Data. In *AGU Fall Meeting Abstracts B33C-0191*; American Geophysical Union: Washington, DC, USA, 2014.
66. Zarco-Tejada, P.; Hornero, A.; Hernández-Clemente, R.; Beck, P. Understanding the temporal dimension of the red-edge spectral region for forest decline detection using high-resolution hyperspectral and Sentinel-2a imagery. *ISPRS J. Photogramm. Remote Sens.* **2018**, *137*, 134–148. [[CrossRef](#)] [[PubMed](#)]
67. Young, C.J.; Liu, S.; Schumacher, J.A.; Schumacher, T.E.; Kaspar, T.C.; McCarty, G.W.; Napton, D.; Jaynes, D.B. Evaluation of a model framework to estimate soil and soil organic carbon redistribution by water and tillage using ¹³⁷Cs in two US Midwest agricultural fields. *Geoderma* **2014**, *232*, 437–448. [[CrossRef](#)]
68. Zhu, M.; Feng, Q.; Zhang, M.; Liu, W.; Qin, Y.; Deo, R.C.; Zhang, C. Effects of topography on soil organic carbon stocks in grasslands of a semiarid alpine region, northwestern China. *J. Soils Sediments* **2019**, *19*, 1640–1650. [[CrossRef](#)]
69. Jacquemoud, S.; Ustin, L. Modeling Leaf Optical Properties. Photobiological Sciences Online. 2008. Available online: http://photobiology.info/Jacq_Ustin.html (accessed on 18 October 2021).
70. Liu, X.; Trogisch, S.; He, J.-S.; Niklaus, P.A.; Bruelheide, H.; Tang, Z.; Erfmeier, A.; Scherer-Lorenzen, M.; Pietsch, K.A.; Yang, B. Tree species richness increases ecosystem carbon storage in subtropical forests. *Proc. R. Soc. B* **2018**, *285*, 20181240. [[CrossRef](#)] [[PubMed](#)]
71. Waring, R.; Landsberg, J.; Williams, M. Net primary production of forests: A constant fraction of gross primary production? *Tree Physiol.* **1998**, *18*, 129–134. [[CrossRef](#)]
72. Hong, T.; Lin, H.; He, D. Characteristics and correlations of leaf stomata in different *Aleurites montana* provenances. *PLoS ONE* **2018**, *13*, e0208899. [[CrossRef](#)] [[PubMed](#)]
73. Myneni, R.B.; Ramakrishna, R.; Nemani, R.; Running, S.W. Estimation of global leaf area index and absorbed PAR using radiative transfer models. *IEEE Trans. Geosci. Remote Sens.* **1997**, *35*, 1380–1393. [[CrossRef](#)]